

A TWO-STAGE GLOBALLY-DIVERSE ADVERSARIAL ATTACK FOR VISION-LANGUAGE PRE-TRAINING MODELS

Wutao Chen¹, Huaqin Zou¹, Chen Wan^{1*}, Lifeng Huang²

¹Department of Computer Science and Technology, Shantou University, Shantou, China

²College of Mathematics and Informatics, South China Agricultural University, Guangzhou, China

ABSTRACT

Vision-language pre-training (VLP) models are vulnerable to adversarial examples, particularly in black-box scenarios. Existing multimodal attacks often suffer from limited perturbation diversity and unstable multi-stage pipelines. To address these challenges, we propose 2S-GDA, a two-stage globally-diverse attack framework. The proposed method first introduces textual perturbations through a globally-diverse strategy by combining candidate text expansion with globally-aware replacement. To enhance visual diversity, image-level perturbations are generated using multi-scale resizing and block-shuffle rotation. Extensive experiments on VLP models demonstrate that 2S-GDA consistently improves attack success rates over state-of-the-art methods, with gains of up to 11.17% in black-box settings. Our framework is modular and can be easily combined with existing methods to further enhance adversarial transferability.

Index Terms— Adversarial Attack, VLP Models, Multi-modal Retrieval, Transferability

1. INTRODUCTION

Vision-language pre-training (VLP) models have achieved impressive performance across a wide range of multimodal tasks, such as image-text retrieval [1] and visual question answering [2]. Despite their success, recent studies [3, 4] have revealed that these models are vulnerable to adversarial examples. By introducing small perturbations to either the image, the text, or both modalities, adversarial examples can disrupt multimodal semantic alignment and lead to substantial performance degradation [5, 6]. Moreover, adversarial examples generated by a surrogate model can remain effective in black-box settings, revealing their cross-model transferability [7, 8]. This property poses a practical threat in black-box scenarios and has attracted growing attention [9].

To enhance adversarial transferability in multimodal settings, recent works have explored joint perturbation strategies over image-text pairs. Co-Attack [3] performs coordinated optimization on single pairs, achieving strong white-box per-

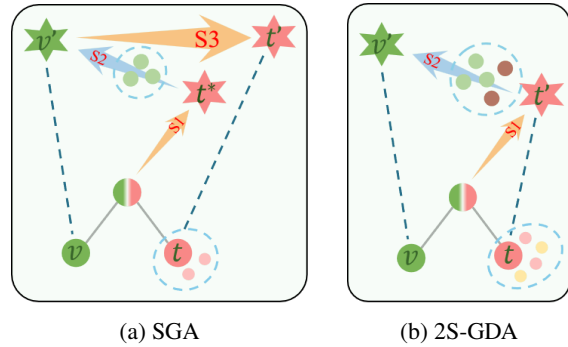


Fig. 1: Comparison of cross-modal interactions. (a) **SGA**: three-stage perturbation (S1: text \rightarrow S2: image \rightarrow S3: text). (b) **2S-GDA**: two-stage perturbation (S1: text \rightarrow S2: image). v : input image; t : paired caption; t^* : intermediate state; v' , t' : corresponding adversarial examples. Arrows indicate guidance for generating adversarial examples.

formance but limited transferability due to insufficient diversity. Set-level Guidance Attack (SGA) [4] addresses this issue by introducing a three-stage framework with set-level textual optimization and multi-scale image augmentations. Wang et al. [10] incorporate BSR (block shuffling and rotation) augmentation strategy [11] into SGA to enhance visual perturbations. DRA [8] enriches adversarial trajectories through multi-step perturbation modeling, and SA-AET [7] leverages adaptive augmentations to improve transferability.

However, two key limitations remain that may hinder the effectiveness of existing approaches. First, as illustrated in Fig. 1a, the representative framework SGA [4] adopts a three-stage pipeline (S1: text \rightarrow S2: image \rightarrow S3: text), where an initial discrete textual perturbation is followed by continuous image perturbation and a final round of text modification. The final stage often introduces semantic drift, which can undermine the effectiveness of earlier gains. As shown in Fig. 2a, the attack success rate (ASR) of S2 generally exceeds that of S3, demonstrating that the last-stage modification degrades overall effectiveness. We compute the probability density distributions (PDD) of Euclidean distance and cosine similarity in feature space between the original input and the adversarial examples generated by S2 and S3. As shown in Figs. 2b and 2c, adversarial examples from S3 are closer to the origi-

*Corresponding author.

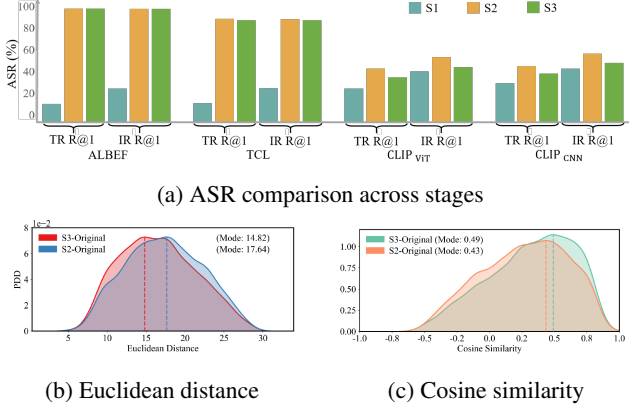


Fig. 2: Feature-space analysis of SGA.

nal input in the feature space, with a lower Euclidean distance (14.82 vs. 17.64) and higher cosine similarity (0.49 vs. 0.43), indicating reduced feature-level deviation and weaker perturbation (as detailed in the supplementary material). Second, most existing methods rely on greedy substitution strategies that select only the top-1 token from BERT-MLM [12] predictions. This heuristic overlooks the semantic contributions of non-key tokens and constrains the exploration of a more globally diverse perturbation space.

To address these challenges, we propose **2S-GDA (Two-Stage Globally-Diverse Attack)**, a new attack framework that improves transferability by rethinking both the attack pipeline structure and the semantic perturbation mechanism. As illustrated in Fig. 1b, 2S-GDA restructures the process into two stages, avoiding the unstable re-perturbation of the text. Specifically, we introduce a globally-aware textual perturbation module that constructs a multi-source candidate pool using BERT-MLM and WordNet [13], and selects replacements by jointly considering token importance and cross-modal alignment loss. In parallel, a visual perturbation module applies multi-scale resizing and BSR [11] to enhance the diversity and effectiveness of image-level adversarial perturbations. Extensive experiments on VLP models demonstrate that 2S-GDA consistently outperforms state-of-the-art baselines, particularly in black-box settings. Moreover, the proposed framework is modular and extensible, and can be easily integrated into existing methods to further enhance adversarial transferability. We summarize our contributions as follows.

- We propose 2S-GDA, a new two-stage attack framework that eliminates the instability introduced by repeated textual perturbations.
- We design a globally-aware textual perturbation mechanism that expands candidate space and avoids local greedy traps.
- Extensive experiments demonstrate that our method consistently outperforms state-of-the-art baselines, especially under black-box settings.

2. METHODOLOGY

2.1. Notations

Let (v, t) denote an image-text pair sampled from a multi-modal dataset \mathcal{D} . In VLP models, we denote the image encoder as $\mathcal{F}_I(\cdot)$, the text encoder as $\mathcal{F}_T(\cdot)$, and the multimodal fusion module as $\mathcal{F}_M(\cdot)$. Specifically, the image and text embeddings are obtained as $e_v = \mathcal{F}_I(v)$ and $e_t = \mathcal{F}_T(t)$, respectively. The fused multimodal representation is then computed as $\mathcal{F}_M(e_v, e_t)$.

We define $\mathcal{B}[v, \varepsilon_v]$ and $\mathcal{B}[t, \varepsilon_t]$ as the adversarial search spaces for the image and text modalities, respectively. Here, ε_v denotes the maximum allowable perturbation magnitude (e.g., ℓ_∞ norm bound), and ε_t denotes the maximum number of token substitutions permitted within the caption. The goal is to craft adversarial examples $(v', t') \in \mathcal{B}[v, \varepsilon_v] \times \mathcal{B}[t, \varepsilon_t]$ such that the fused multimodal embedding $\mathcal{F}_M(\mathcal{F}_I(v'), \mathcal{F}_T(t'))$ becomes misaligned with the clean representation, resulting in incorrect retrieval results.

2.2. Two-Stage Attack Pipeline

To overcome the limitations of existing three-stage frameworks (e.g., SGA), 2S-GDA introduces a streamlined two-stage pipeline that removes the unstable textual re-perturbation phase while retaining both semantic guidance and perturbation diversity. The proposed framework consists of the following two core stages.

Stage I: Textual Perturbation

Given a caption t , we utilize its paired image encoding $\mathcal{F}_I(v)$ as cross-modal supervision to identify a subset of critical words $t' = \{t'_1, t'_2, \dots, t'_M\}$ that are most crucial for cross-modal matching. For each selected token, a set of candidate replacements is generated using a Masked Language Model (MLM). The objective is to reduce the semantic consistency between the perturbed text and the original image by minimizing the cosine similarity between the perturbed text embedding $\mathcal{F}_T(t')$ and the original image features $\mathcal{F}_I(v)$:

$$t' = \arg \max_{t' \in \mathcal{B}[t, \varepsilon_t]} \left(-\frac{\mathcal{F}_T(t') \cdot \mathcal{F}_I(v)}{\|\mathcal{F}_T(t')\| \|\mathcal{F}_I(v)\|} \right) \quad (1)$$

where \mathcal{F}_T and \mathcal{F}_I denote the text and image encoders, respectively. The adversarial caption t' is optimized to be maximally distant from the original image v in the embedding space.

Stage II: Visual Perturbation

In this stage, the goal is to introduce adversarial perturbations to the image v such that the resulting visual embedding $\mathcal{F}_I(v')$ is misaligned with the adversarial text t' obtained in Stage I. To increase attack generalization, we apply a set of transformation-based augmentations, including multi-scale resizing and BSR, to construct a diverse image set \mathcal{S}_v for adversarial optimization. The adversarial image v' is generated

by solving the following optimization problem:

$$v' = \operatorname{argmax}_{v' \in B[v, \varepsilon_v]} - \sum_{i=1}^M \frac{\mathcal{F}_T(t'_i)}{\|\mathcal{F}_T(t'_i)\|} \sum_{v_i \in S_v} \frac{\mathcal{F}_I(v_i)}{\|\mathcal{F}_I(v_i)\|} \quad (2)$$

where S_v denotes the set of image variants generated by applying BSR and multi-scale resizing to v' , and each $v_i \in S_v$ is obtained by scaling v' with a factor s_i . This objective encourages all $v_i \in S_v$ to remain semantically distant from adversarial captions t'_i in the embedding space.

2.3. Globally-Diverse Strategy

To increase semantic diversity and avoid overfitting to the top-1 token, a Globally-Diverse Strategy is introduced, consisting of two components.

1) *Candidate Text Expansion (CTE)*. Since standard MLMs provide limited variations, WordNet is incorporated to build a multi-source candidate pool. For each token w selected for perturbation, the top- k predictions from BERT-MLM ($C_{\text{MLM}}(w)$) are combined with synonyms from WordNet ($C_{\text{WN}}(w)$). The final candidate set excludes invalid items such as stopwords, subword fragments, and special symbols,

$$C(w) = \{c \in C_{\text{MLM}}(w) \cup C_{\text{WN}}(w) \mid c \neq R\} \quad (3)$$

where R denotes the set of excluded items. This expansion enlarges the perturbation space while preserving semantic plausibility.

2) *Globally-Aware Replacement (GAR)*. We employ a global scoring mechanism to evaluate the impact of candidate substitutions on cross-modal alignment. Specifically, the top- k most influential tokens in the input text t are identified by gradient-based saliency scoring on a masked language model (MLM), forming the set $W_{\text{imp}} = \{w_1, w_2, \dots, w_k\}$, where k is the number of influential tokens. For each $w_i \in W_{\text{imp}}$, the candidate set $C(w_i)$ is constructed according to Eq. (3). Each candidate token $\tilde{w} \in C(w_i)$ is then substituted into t , and the corresponding adversarial loss $\mathcal{J}(v, t : w_i \rightarrow \tilde{w})$ is computed. We select the token–candidate pair that yields the maximum adversarial loss,

$$(w'_i \rightarrow \tilde{w}') = \arg \max_{\substack{w_i \in W_{\text{imp}} \\ \tilde{w} \in C(w_i)}} \mathcal{J}(v, t : w_i \rightarrow \tilde{w}) \quad (4)$$

where W_{imp} denotes the set of important tokens and $C(w_i)$ represents the candidate pool for w_i . Note that although k influential tokens are initially selected, only ε_t token with the highest alignment disruption is ultimately replaced. This selective strategy preserves semantic stability and mitigates excessive semantic drift.

The detailed 2S-GDA algorithm is provided in the supplementary material. Compared to existing methods (e.g., SGA and its variants), our approach removes the unstable text re-perturbation stage and introduces globally-diverse textual augmentation, resulting in more semantically consistent and transferable adversarial examples.

Table 1: ASR (%) of our method and the baseline approaches. Diagonal entries indicate white-box attacks.

Source	Attack	ALBEF		TCL		CLIP _{VIT}		CLIP _{CNN}	
		TR R@1	IR R@1	TR R@1	IR R@1	TR R@1	IR R@1	TR R@1	IR R@1
ALBEF	SGA [4]	100.00	99.95	89.67	89.64	39.14	47.87	42.66	52.14
	SGA-BSR [10]	100.00	99.95	94.20	94.33	63.68	70.01	71.26	73.34
	DRA [8]	99.90	99.93	91.68	91.86	47.12	57.18	51.72	60.07
	SA-AET [7]	99.90	99.98	96.42	96.02	55.58	63.89	57.22	65.59
2S-GDA (ours)	100.00	100.00	97.26	96.40	74.85	78.77	77.01	81.34	
	SGA [4]	92.60	92.96	100.00	100.00	37.91	48.16	42.91	52.80
	SGA-BSR [10]	96.66	96.66	100.00	99.95	64.66	69.33	69.99	74.58
	TCL	94.68	95.28	100.00	99.95	47.61	57.54	51.85	62.06
	SA-AET [7]	98.85	98.50	100.00	100.00	56.20	63.47	59.77	67.86
CLIP _{VIT}	2S-GDA (ours)	97.50	98.13	100.00	100.00	73.37	79.48	78.67	83.70
	SGA [4]	22.73	35.69	25.29	37.19	100.00	100.00	55.56	62.06
	SGA-BSR [10]	49.64	59.19	51.63	58.38	100.00	100.00	83.52	84.67
	DRA [8]	29.20	44.34	31.09	45.19	100.00	100.00	65.64	70.33
	SA-AET [7]	36.60	50.44	39.20	51.10	100.00	100.00	71.01	74.10
CLIP _{CNN}	2S-GDA (ours)	54.54	65.18	55.43	65.45	100.00	99.97	90.04	89.98
	SGA [4]	15.54	29.58	18.12	32.57	42.58	52.71	99.87	99.97
	SGA-BSR [10]	24.19	36.97	26.13	40.86	52.15	61.08	100.00	99.93
	DRA [8]	19.50	34.47	21.18	37.71	48.34	59.79	100.00	99.97
	SA-AET [7]	23.98	38.28	27.29	41.81	54.11	64.21	100.00	99.97
2S-GDA (ours)	28.78	46.02	34.35	49.05	67.61	75.19	100.00	99.90	

3. EXPERIMENTS

3.1. Experimental Settings

Datasets. Experiments are conducted on the Flickr30K dataset [14], which contains 1000 images with five human-annotated captions each. Additional results on the MSCOCO dataset are provided in the supplementary material¹.

Models. Two types of VLP model are selected, i.e., fused and aligned. ALBEF [15] and TCL [2] represent fused models, while CLIP_{VIT} and CLIP_{CNN} [16] serve as aligned models.

Baselines. We compare our approach with four recent attack methods, i.e., SGA [4], SGA-BSR [10], DRA [8], and SA-AET [7], as well as their combined variants (DRA-BSR and SA-AET-BSR). Earlier methods such as PGD [17], BERT-Attack [18], Sep-Attack, and Co-Attack [3] are reported in the supplementary material.

Attack Settings. Following [7, 8], image perturbations are generated using PGD with $\varepsilon_v = 8/255$, step size $2/255$, and $T = 10$ iterations. For the text modality, we adopt BERT-Attack [18] with a perturbation bound $\varepsilon_t = 1$, a candidate list size of $W = 10$, and $k = 3$ influential tokens.

Metrics. The effectiveness of adversarial attacks is evaluated using the Attack Success Rate (ASR) measured on Rank-1 retrieval accuracy, including both text-to-image (TR R@1) and image-to-text (IR R@1) tasks.

3.2. Experimental Results

Table 1 reports the ASR (%) of our proposed 2S-GDA and four baselines (SGA, SGA-BSR, DRA, and SA-AET). Diagonal entries indicate white-box attacks, and off-diagonal entries reflect transferability. Compared to baselines, 2S-GDA

¹The code and supplementary material are available at <https://github.com/chenwutao123/2S-GDA>.

Table 2: ASR (%) of our method combined with baseline methods. The adversarial examples are generated by ALBEF.

Attack	ALBEF		TCL		CLIP _{ViT}		CLIP _{CNN}	
	TR R@1	IR R@1	TR R@1	IR R@1	TR R@1	IR R@1	TR R@1	IR R@1
DRA-BSR	99.79	99.93	91.04	91.33	46.75	57.25	50.45	59.59
2S-GDA-DRA (ours)	100.00	100.00	93.78	94.07	52.64	64.21	56.58	67.10
SA-AET-BSR	99.79	99.95	96.21	96.21	75.21	79.54	77.14	80.27
2S-GDA-SA-AET (ours)	100.00	99.93	98.00	97.88	80.98	84.89	81.61	84.36

Original		<ul style="list-style-type: none"> Two men and a woman pose with signs for Obama and Chris Gregoire. Three people pose with their political signs out in public. Three democrat supporters hold signs for an election. Three people smiling and holding political signs. Three people with political signs.
SGA-BSR		<ul style="list-style-type: none"> Two men and a woman song with signs for Obama and Chris Gregoire. ✓ Different people pose with their political signs out in public. ✓ Votes democrat supporters hold signs for an election. ✓ ... people smiling and holding political signs. ✓ People people with political signs. ✓
2S-GDA		<ul style="list-style-type: none"> Two men and a woman pose with mansion for Obama and Chris Gregoire. ✓ Three people lay with their political signs out in public. ✗ Three democrat supporters hold mansion for an election. ✗ ... people smiling and holding political signs. ✓ Three mass with political signs. ✗

Fig. 3: Visualization of adversarial examples on the image-text retrieval task (ALBEF \rightarrow CLIP_{ViT}).

generally achieves 100% ASR in white-box settings, and consistently outperforms them in black-box settings, with improvements of $0.11\% \sim 11.17\%$. These results demonstrate the effectiveness of our method in enhancing adversarial transferability.

To evaluate the extensibility of our method, we integrate 2S-GDA into two baseline frameworks (DRA and SA-AET). Table 2 demonstrates that our method consistently achieves 1.57% to 7.51% higher ASR than the baselines in black-box settings.

In addition, several visualization results are provided. Fig. 3 presents a visual comparison between SGA-BSR and our method on the image-text retrieval task. The notation “Model A \rightarrow Model B” denotes that adversarial examples are generated by “Model A” and then evaluated on “Model B”. The red text indicates the modified words, while the red crosses and green checks denote incorrect and correct retrieval matches, corresponding to successful and failed attacks, respectively. The results demonstrate that 2S-GDA more effectively disrupts visual-text alignment. Fig. 4 highlights the salient regions for the word “boy” using ALBEF on clean and adversarial images. Compared to baselines, 2S-GDA shifts attention away from the correct region, demonstrating stronger interference with semantic alignment.

3.3. Ablation Studies

Firstly, we perform ablation studies to assess the impact of the proposed components: the two-stage pipeline (2S), Candidate Text Expansion (CTE), and Globally-Aware Replace-

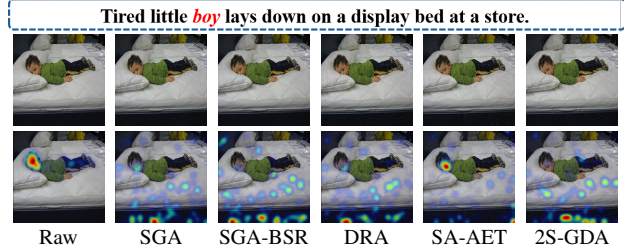


Fig. 4: Visualization of clean vs. adversarial examples. Rows show captions, images, and salient regions for “boy”.

Table 3: Ablation results of different modules on image-text retrieval across three attack frameworks.

	SGA-BSR		DRA-BSR		SA-AET-BSR	
	TR R@1	IR R@1	TR R@1	IR R@1	TR R@1	IR R@1
w/o 2S	64.91	70.94	53.50	62.50	80.25	84.66
w/o CTE	71.90	75.55	49.08	59.79	77.67	81.12
w/o GAR	71.66	76.90	52.39	62.18	79.63	81.86
Completed	74.72	79.64	52.64	64.21	80.98	84.89

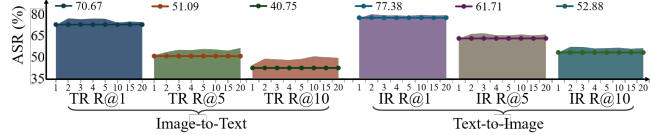


Fig. 5: Comparison of attack success rates under different number of influential tokens k in GAR, with the baseline (w/o GAR) included for reference (ALBEF \rightarrow CLIP_{ViT}).

ment (GAR). As shown in Table 3, removing any module leads to a noticeable performance drop, confirming their effectiveness and complementarity. Among them, excluding 2S causes the most significant degradation, highlighting the importance of avoiding repeated textual perturbation.

Secondly, we study the effect of the influential tokens k in GAR. Fig. 5 presents the results on ALBEF \rightarrow CLIP_{ViT}, while the results on ALBEF \rightarrow TCL and ALBEF \rightarrow CLIP_{CNN} are provided in Fig. A4 of the supplementary material. As observed, the ASR peaks around $k = 3$ and then declines, which may be attributed to excessive semantic distortion.

4. CONCLUSION

In this work, we propose 2S-GDA, a two-stage attack framework by introducing the globally-diverse strategy. Extensive experiments demonstrate that 2S-GDA consistently outperforms state-of-the-art baselines, particularly in black-box settings. Moreover, our proposed framework exhibits better extensibility and can be easily combined with existing methods to further improve transferability.

5. REFERENCES

- [1] Zaid Khan and Yun Fu, “Exploiting bert for multimodal target sentiment classification through input space translation,” in *Proceedings of ACM International Conference on Multimedia (ACM MM)*, 2021, pp. 3034–3042.
- [2] Jinyu Yang, Jiali Duan, Son Tran, Yi Xu, Sampath Chanda, Liqun Chen, Belinda Zeng, Trishul Chilimbi, and Junzhou Huang, “Vision-language pre-training with triple contrastive learning,” in *Proceedings of IEEE Conference on Computer Vision and Pattern Recognition (CVPR)*, 2022, pp. 15671–15680.
- [3] Jiaming Zhang, Qi Yi, and Jitao Sang, “Towards adversarial attack on vision-language pre-training models,” in *Proceedings of ACM International Conference on Multimedia (ACM MM)*, 2022, pp. 5005–5013.
- [4] Dong Lu, Zhiqiang Wang, Teng Wang, Weili Guan, Hongchang Gao, and Feng Zheng, “Set-level guidance attack: Boosting adversarial transferability of vision-language pre-training models,” in *Proceedings of IEEE International Conference on Computer Vision (ICCV)*, 2023, pp. 102–111.
- [5] Yue Xu, Xin Liu, Kun He, Shao Huang, Yaodong Zhao, and Jie Gu, “Image mixing and gradient smoothing to enhance the sar image attack transferability,” in *Proceedings of IEEE International Conference on Acoustics, Speech and Signal Processing (ICASSP)*, 2024, pp. 5380–5384.
- [6] Fengfan Zhou, Hefei Ling, Yuxuan Shi, Jiazhong Chen, and Ping Li, “Improving visual quality and transferability of adversarial attacks on face recognition simultaneously with adversarial restoration,” in *Proceedings of IEEE International Conference on Acoustics, Speech and Signal Processing (ICASSP)*, 2024, pp. 4540–4544.
- [7] Xiaojun Jia, Sensen Gao, Qing Guo, Simeng Qin, Ke Ma, Yihao Huang, Yang Liu, Ivor Tsang, and Xiaochun Cao, “Semantic-aligned adversarial evolution triangle for high-transferability vision-language attack,” *IEEE Transactions on Pattern Analysis and Machine Intelligence*, vol. 47, no. 10, pp. 8489–8505, 2025.
- [8] Sensen Gao, Xiaojun Jia, Xuhong Ren, Ivor Tsang, and Qing Guo, “Boosting transferability in vision-language attacks via diversification along the intersection region of adversarial trajectory,” in *Proceedings of European Conference on Computer Vision (ECCV)*, 2024, pp. 442–460.
- [9] Haochen Luo, Jindong Gu, Fengyuan Liu, and Philip Torr, “An image is worth 1000 lies: Adversarial transferability across prompts on vision-language models,” in *Proceedings of International Conference on Learning Representations (ICLR)*, 2024.
- [10] Wenbin Wang, Siyuan Gao, Manda Gao, Ling Liang, Guangjun Yang, Bangyan He, and Yaozu Liu, “Improving adversarial transferability on vision-language pre-training models via block shuffle and rotation,” *Frontiers of Data and Computing*, vol. 7, no. 02, pp. 130–140, 2025.
- [11] Kunyu Wang, Xuanran He, Wenxuan Wang, and Xiaosen Wang, “Boosting adversarial transferability by block shuffle and rotation,” in *Proceedings of IEEE Conference on Computer Vision and Pattern Recognition (CVPR)*, 2024, pp. 24336–24346.
- [12] Jacob Devlin, Ming-Wei Chang, Kenton Lee, and Kristina Toutanova, “Bert: Pre-training of deep bidirectional transformers for language understanding,” in *Proceedings of Conference of the North American Chapter of the Association for Computational Linguistics: Human Language Technologies (NAACL-HLT)*, 2019, pp. 4171–4186.
- [13] George A Miller, “Wordnet: a lexical database for english,” *Communications of the ACM*, vol. 38, no. 11, pp. 39–41, 1995.
- [14] Bryan A Plummer, Liwei Wang, Chris M Cervantes, Juan C Caicedo, Julia Hockenmaier, and Svetlana Lazebnik, “Flickr30k entities: Collecting region-to-phrase correspondences for richer image-to-sentence models,” in *Proceedings of IEEE International Conference on Computer Vision (ICCV)*, 2015, pp. 2641–2649.
- [15] Junnan Li, Ramprasaath Selvaraju, Akhilesh Gotmare, Shafiq Joty, Caiming Xiong, and Steven Chu Hong Hoi, “Align before fuse: Vision and language representation learning with momentum distillation,” *Advances in Neural Information Processing Systems (NeurIPS)*, vol. 34, pp. 9694–9705, 2021.
- [16] Alec Radford, Jong Wook Kim, Chris Hallacy, Aditya Ramesh, Gabriel Goh, Sandhini Agarwal, Girish Sastry, Amanda Askell, Pamela Mishkin, Jack Clark, et al., “Learning transferable visual models from natural language supervision,” in *Proceedings of International Conference on Machine Learning (ICML)*, 2021, pp. 8748–8763.
- [17] Aleksander Madry, Aleksandar Makelov, Ludwig Schmidt, Dimitris Tsipras, and Adrian Vladu, “Towards deep learning models resistant to adversarial attacks,” in *Proceedings of International Conference on Learning Representations (ICLR)*, 2017.
- [18] Linyang Li, Ruotian Ma, Qipeng Guo, Xiangyang Xue, and Xipeng Qiu, “Bert-attack: Adversarial attack against bert using bert,” in *Proceedings of Conference on Empirical Methods in Natural Language Processing (EMNLP)*, 2020, pp. 6193–6202.